University of Arkansas, Fayetteville

ScholarWorks@UARK

Physics Undergraduate Honors Theses | Physics

5-2022

Emergent Spectra of Young X-Ray Emitting Populations Across Environments

Alex Siebenmorgen
University of Arkansas, Fayetteville

Follow this and additional works at: https://scholarworks.uark.edu/physuht

Part of the External Galaxies Commons, Physics Commons, and the Stars, Interstellar Medium and the Galaxy Commons

Citation

Siebenmorgen, A. (2022). Emergent Spectra of Young X-Ray Emitting Populations Across Environments. *Physics Undergraduate Honors Theses* Retrieved from https://scholarworks.uark.edu/physuht/11

This Thesis is brought to you for free and open access by the Physics at ScholarWorks@UARK. It has been accepted for inclusion in Physics Undergraduate Honors Theses by an authorized administrator of ScholarWorks@UARK. For more information, please contact scholar@uark.edu, uarepos@uark.edu.

EMERGENT SPECTRA OF YOUNG X-RAY EMITTING POPULATIONS ACROSS ENVIRONMENTS

An Honors Thesis submitted in partial fulfillment of the requirements for Honors Studies in Physics

By

Alex Siebenmorgen

Spring 2022

Physics

J. William Fulbright College of Arts and Sciences

The University of Arkansas

Acknowledgements

I would like to acknowledge Dr. Bret Lehmer in the Department of Physics for guiding me in the writing of this Honors Thesis, as well as for helping me develop my ability in physics and astronomy. I would also like to acknowledge Dr. Daniel Kennefick, Dr. Barry Ward, and Sean Morrissey for serving on my thesis committee.

Table of Contents

Abstract

We construct reasonably accurate models of the X-Ray spectra of a multitude of sources in M51. We construct both average and individual models for the sources, which are split into 16 groups as the counts per source increases. Then, we create a plot to show how the model-predicted values of column density (nH) and photon index (Γ) change with luminosity. These models will be used to create an accurate X-Ray stellar energy distribution (SED) for M51, and to better understand how the SED changes with environmental factors like metallicity and star formation rate (SFR).

Introduction

In a relatively short time after the Big Bang, the collapse of large gas clouds resulted in the formation of the first stars. The most massive of these stars formed

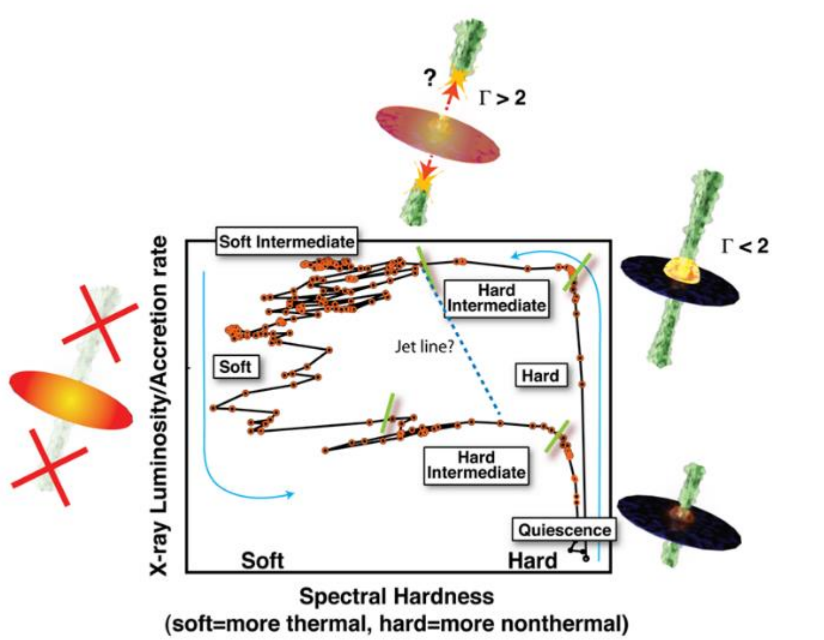

Figure 1: Plot of accretion states and how the binary system and its spectrum changes (Markoff, 2020). The cycle follows the blue arrow.

compact objects such as black holes and neutron stars. A small percentage of the black holes and neutron stars that came into existence due to stellar death became a part of X-Ray binary systems. In these systems, the compact object and a non-collapsed star orbit each other, and the compact object accretes mass from the non-collapsed star, forming an accretion disk (Shakura & Sunyaev, 1973). The matter in the accretion disk is heated to tens of millions of degrees by viscous forces, causing it to emit powerful X-Rays. These X-Rays and the binary systems are thought to have had a significant effect on the structure and formation of galaxies, stars, and planets throughout the universe as we know it. Properties of X-Ray binaries are linked to galactic properties such as galactic metallicity, or the presence of elements more massive than hydrogen and helium, and the mass of stars (Vulic et al., 2018). Moreover, X-ray emission likely increased gas temperature throughout the universe, affecting subsequent large-scale-structure and star formation.

It is well known that accreting X-Ray binary systems undertake multiple accretion states in which they exhibit a variety of different properties depending on the rate of matter being accreted (Vulic et al., 2018). This includes changes in jet emission, disk size, and luminosity, as seen in Figure 1. Historically, our understanding of X-ray binaries has come from studying older, low-mass systems in the Milky Way, which has a relatively low star formation rate and does not provide a complete picture of the binary systems present in other galaxies. Many sources in nearby galaxies with high star formation rates are younger and higher mass than those found in the Milky Way, and would exhibit accretion states that likely do not vary in the same way. An X-ray binary's form, activity, and spectrum change dramatically as it passes from state to state (Done et al., 2007). Thus, the accuracy of spectral models for galaxies outside of the Milky Way relies heavily on identifying the accretion states of the binary populations contained in them. The accuracy of spectral models further depends on incorporating data from galaxies with distinct properties from that of the Milky Way.

Motivation

The goal of this research project is to use Chandra X-Ray Observatory data to construct a realistic model of the X-ray Stellar Energy Distribution (SED) for high-mass X-ray binary point sources in M-51 (shown in Figure 3). We will construct these to show how the SED changes based on star formation rate and metallicity. The process described here involves finding the best-fit models for the column density and power-law slope, which is an essential step in constructing these SEDs. At the end of this process, we will be able to put together a more complete picture of the effect that certain galactic environments have on the ionization potential of high-mass X-ray binaries (HMXBs) (Lehmer et al., 2016). The spectrum is focused within the 0.5-8 keV spectral range, as there would be sufficient resolution to distinguish the source radiation from the background radiation in this range.

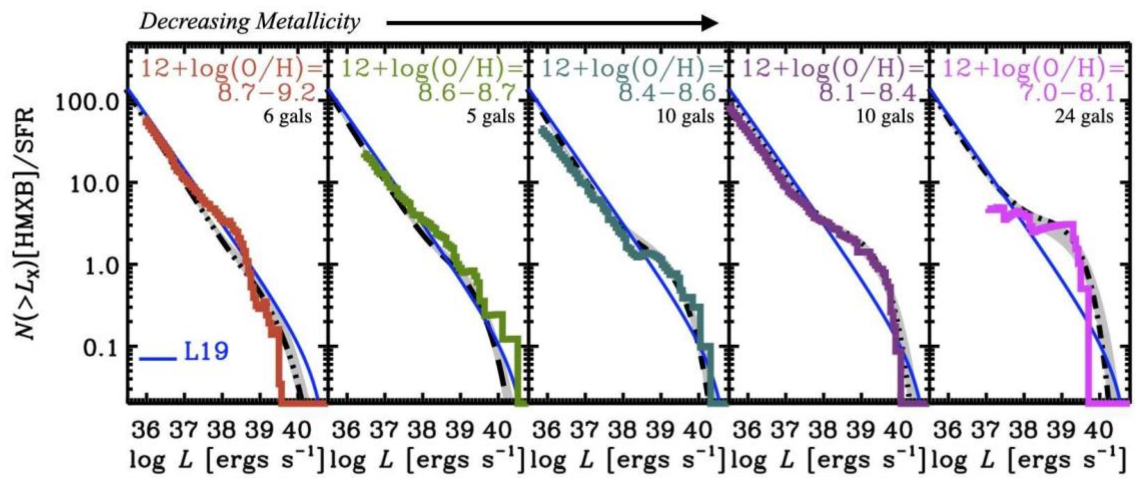

Figure 2: SFR-normalized HMXB XLFs with varying metallicity. The effect that metallicity has on the HMXB XLF is clearly shown here, given the subtraction of other model components that might affect the XLF (Lehmer, et al., 2021). Plot retrieved from (Lehmer, et al., 2021).

The galaxies on which we based this study are young star-forming galaxies, which were selected from a variety of environments with varying metallicities. The X-ray spectrum of these galaxies is heavily affected by the HMXBs contained within them, which each have varying properties. For example, they can be composed of different compact objects or be in different accretion states. As a result, the individual spectrum of these sources can be immensely diverse across the target spectral range. In addition to the compact object and the accretion states, it is also expected that metallicity (Douna, V. M. et al., 2015; Brorby, M. et al., 2016; Fornasini, F. M. et al., 2020) and star formation rate (Lehmer, B. D. et al., 2010; Mineo, S., et al., 2012) in the surrounding area would heavily impact the SED. The effect of metallicity on the HMXB X-Ray Luminosity Function (XLF) is shown in Figure 2. Examining the extent to which the metallicity and star formation rate affect the SED of a source is fundamental to the goal of this project, and it would allow me to build more accurate models of the SEDs of

HMXBs across the galaxy as a whole while accounting for any variation in metallicity and star formation rate.

This research project gives important information regarding the effect of HMXB emission from high star formation rate galaxies. Specifically, this information would allow us to understand how HMXB emission interacts with the early intergalactic medium, as HMXBs are expected to produce ionizing radiation with much longer path lengths than the UV emission seen in nearby galaxies (Pakull, M. W. et al., 2010; Soria, R. et al., 2010; Lopez, K. M. et al., 2019). This project would give astronomers a better understanding of the spectral shape of emission at higher energy levels and different environments than the Milky Way. The project would also provide observational insight on star formation and galaxy development in the early universe, as the conditions in young galaxies are closely related to the conditions of the young universe. With these spectral models, we can learn much more about the physical properties of the galaxy and how it developed over time. For example, an environment with lower metallicity would be expected to have weaker stellar winds with stars expanding more significantly than an environment with a higher metallicity. This would allow binary system orbits to remain small, resulting in larger mass transfer rates and more numerous and luminous HMXBs (Linden, T., et al. 2010; Fragos, T., et al. 2013; Wiktorowicz, G., etal. 2019). Additionally, recognizing a galaxy with a particularly low age and high star formation rate can provide us with a target for further research and give astronomers knowledge of the quality of data they might receive from that galaxy. It could also supply more information about which accretion states were most prominent in the early universe and how these X-ray binaries affected galactic development. The produced spectra can also be analyzed with the galactic structure in mind to give us new scientific models that explain how the two are related. We could also more accurately gauge the population and characteristics of X-ray sources within a galaxy based on its spectrum with this information.

Procedure

Our approach to this project is to use custom computer programs and statistical modeling techniques to create and evaluate the spectral models. The primary resource we used for this project is archival Chandra X-Ray data, for which PI files were made available from ACISEXTRACT scripts used in an unrelated project (Lehmer et al., 2021). We began by sorting the sources by energy level from lowest to highest. Then, we isolated the sources from the sorted list that were the highest probability sources. To do this, we first excluded all sources within 12 arcseconds from the galactic center to minimize the background noise in the source counts. Then, we excluded the sources with low signal-to-noise ratios, which only have minor contributions to the X-Ray spectrum (Hunt, Q. et al., 2021). We separated these based on (Eq. 1), shown below, where *N* is the number of source counts and *B* is the number of background counts.

$$SNR = \frac{N - B}{\sqrt{N}} \qquad (Eq. 1)$$

This allowed us to model sources for which we had high confidence that the source counts are accurate. Once I isolated the high probability sources, I sorted each source into one of 16 groups. Each source would be added to a group until the total number of counts met or exceeded 1000 and the number of sources met or exceeded 10. This step ensured that I had a sufficient sample from which I could create an accurate stacked model. Examples of sources and how they might be sorted can be found in Figure 4.

Figure 3: Messier 51 (M51, Whirlpool Galaxy). Visible Spectrum. Credit: *NASA, ESA, S. Beckwith (STScI) and the Hubble Heritage Team (STScI/AURA)*

Figure 4: X-Ray image of M51. Sources circled in red would be sorted into one of the lower groups of counts, while sources circled in blue would be sorted into one of the higher groups. Credit: NASA/CXC/Wesleyan Univ./R.Kilgard, et al.

We then began the spectral fitting process with an astrophysical modeling program called Sherpa, using Python as the base programming language to create these computer programs. The main program we used to create the spectral models was designed to take in each count group and to either create an average (stacked) spectral model or a model of the sources withing the group individually. It also provides models for the background counts. We used a power law model as a basis and added multiplicative scale factor and an absorption components to both the stacked and individual models. The absorption was allowed to vary by source in the individual models, whereas a single average absorption was used to fit the stacked model. Then, we added an additive gas component, initially set to a value of 0.2 keV. For the background model, we used a basic linear fit with the addition of an additive gas component.

After we ran this program for each source group, I extracted the model values of column density and photon index. I then ran a program that plotted these values against the luminosity of the source. The values of luminosity were saved in files which corresponded to the sorting of their respective sources. Using these, we can create luminosity and metallicity-dependent probability distribution functions of column density and power-law slope to use in future Monte Carlo simulations.

Results

Select fits from a wide array of energy bins are shown below.

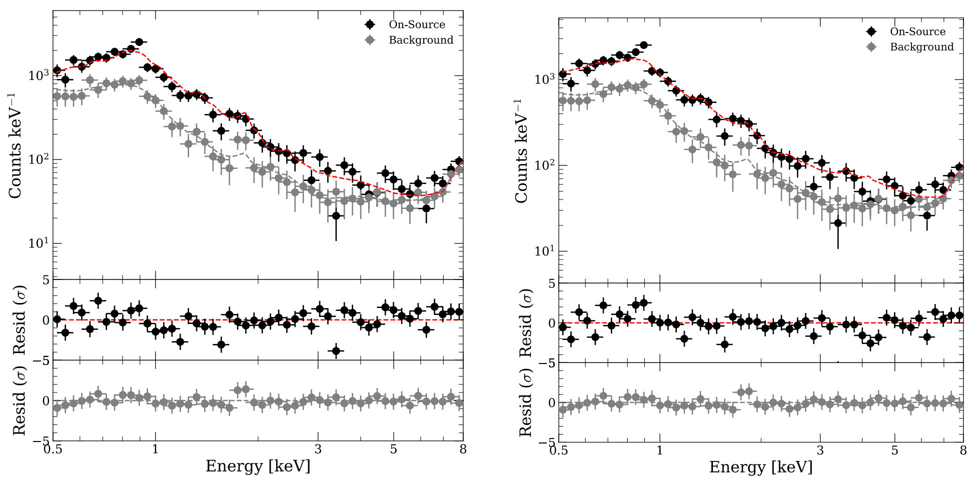

Figure 5: Stacked (left) and individual (right) fits for counts group 1. Notice the small amount of variation from zero in the residuals from both the source counts and the background counts. This gives evidence that both models fit the data well.

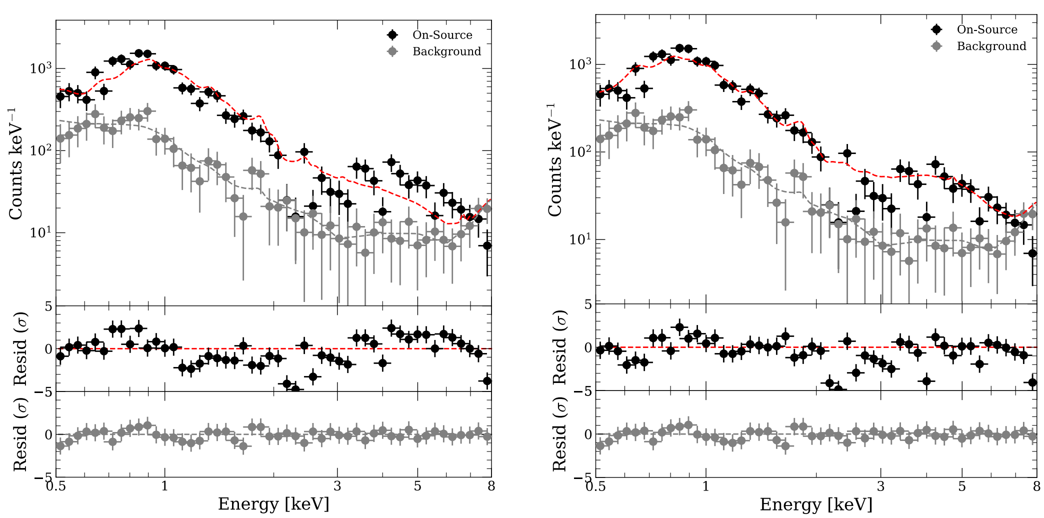

Figure 6: Stacked (left) and individual (right) fits for counts group 7. The residuals for these plots are relatively small, though the individual fits seem slightly better than the stacked fits for this group.

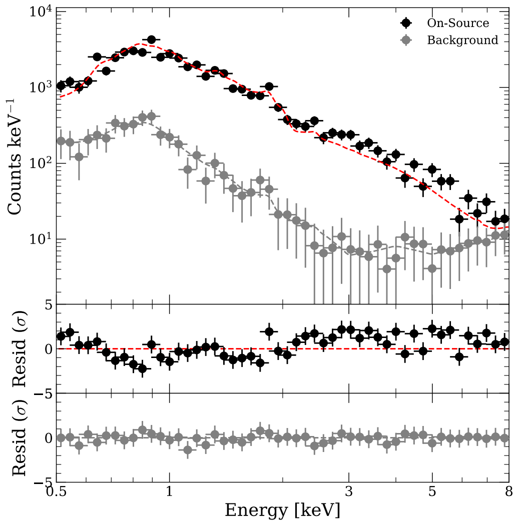

Figure 7: Stacked (left) and individual (right) fits for counts group 12. The individual fit is a slightly better fit for the data, but both are relatively good, nonetheless. The power law slope can certainly be a little bit lower for the stacked it.

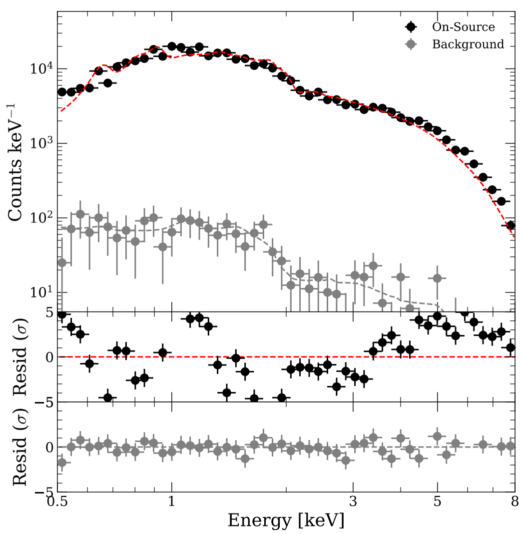

Figure 7: Stacked (left) and individual (right) fit for counts group 16. The residuals have a large amount of variation from zero, though it still seems like the model is a good fit for the data simply from the look of the plot itself. The residuals seem large, but this can perhaps be explained by the larger count values and the differences between them for this count group.

These models, in general, seem to describe the data well. This is evidenced by the low level of variation in the residuals. The fit for group 1 has very little variation from zero. The fit for group 7 had slightly higher, but still not much variation from zero.

The fit for group 16 seem to have a large degree of variation from zero. The stacked fit seems to better describe the data by this metric as the average number of counts per source decreases. However, this standard cannot be used effectively when evaluating the fit of the higher energy sources. This is due to the higher number of counts in the higher energy groups. There is an order of magnitude more counts from the higher energy sources than from the lower energy ones. This means that there will be a larger difference between the number of source counts themselves, resulting in larger residuals in general. However, it can be clearly seen from the upper part of the plot itself that the model describes the sources well. Additionally, the background seems to be consistently well-fit across all sources and groups.

The individual fits, in general, also describe the sources well. These residuals seem consistent with those of the stacked fits, though they are slightly smaller, perhaps as a result of the varying absorption for these fits. The sources dealt with in both are the same, however, so it is expected that the residuals would look about the same, including for the counts 16 group. The background, like the stacked models, looks like it was fit consistently well. Finally, using the modeled column densities and photon indexes, we created the following plots to show how their values change with luminosity.

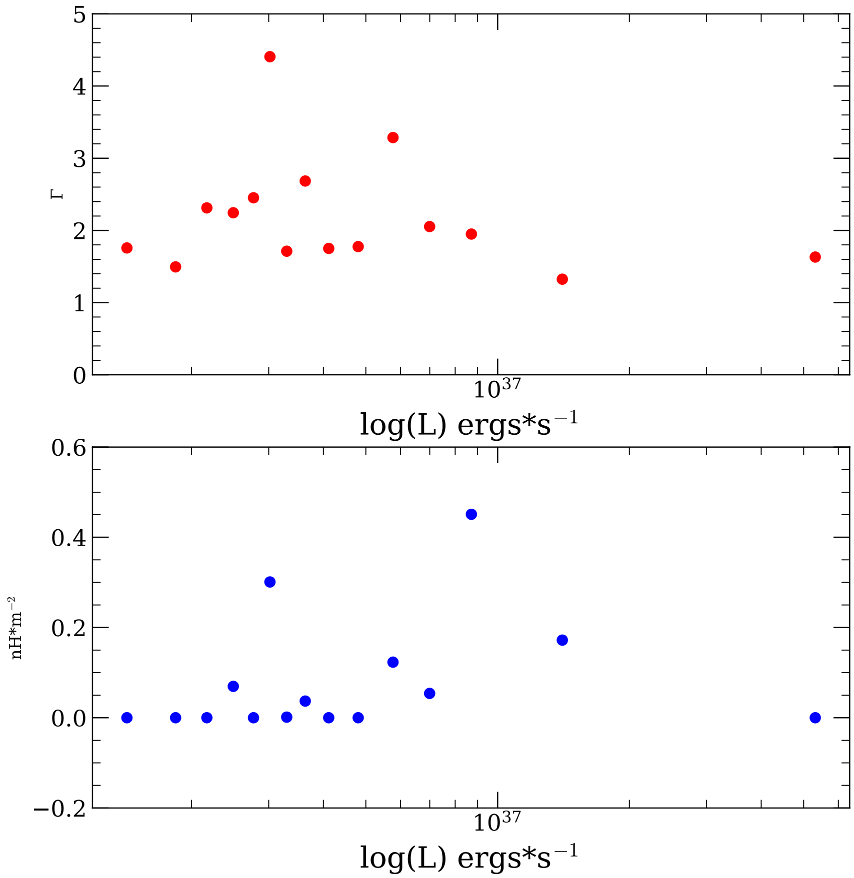

<u>Figure 11</u>: Γ (photon index) and column density (nH) plotted against luminosity. This plot is a reasonable representation, but it will almost certainly change as the project develops, which includes the addition of error bars.

The values reflected in this plot, despite being initial results, reflect reasonable and promising results for the project moving forward. These will certainly be improved in a few ways, which I will specify in the discussion section.

<u>Discussion</u>

These are very much preliminary results, however, the fits seemed accurate overall. One aspect in which the fits might be improved is to further specify the gas component of both models. This could be done by adding an additional absorption component for the gas rather than multiplying it by the general absorption factor. Because these are preliminary results, both the fits and the final plot of nH and Γ will certainly change. In the future, our goal will be to add error bars onto Figure 11 to get a better sense of any trends that exist. Additionally, the spectrum depends on the accretion states of the compact objects and the absorption of their environment (Remillard, R. A. & McClintock, J. E. 2006; Done et al., 2007). Our wide selection of sources with varying properties (BH masses, NS masses & magnetization) allowed us to account for these variables as well, resulting in an accurate assessment of the spectra as a function of luminosity and environmental properties. These sources are also

We also plan to utilize the final plot to create probability distribution functions (PDFs) for the column density and photon index to statistically assess how they vary with luminosity and metallicity. Then, we will use these PDFs to run Monte Carlo simulations for how the X-ray source population spectrum of a galaxy might change given the star formation rate and metallicity. For each simulation, we will then create an XLF for the source and find the young-population SED contribution statistically, which will then be compiled to understand its effect on the overall emergent SED. This procedure will be repeated for sources across a broad range of metallicities and star formation rates, which will allow us to accurately quantify the extent to which the SED depends on these variables.

Conclusion

The preliminary fits for this project described the data well, though they could be improved by adding error bars to identify trends and further specifying the gas component. More analysis is needed to accurately assess the SED's dependence on metallicity and SFR, which includes creating PDFs from the above data and running Monte Carlo simulations. Additionally, this project was focused on young HMXB populations. Upon the completion of this project, more research should be done on how older low mass X-Ray Binaries (LMXBs) and hot gas vary with metallicity and SFR.

References:

1. Brorby, M., et al. 2016, MNRAS, 457, 4081
2. Done, Chris, et al. 2007, arXiv:0708.0148
3. Douna, V. M., et al. 2015, A&A, 579, A44
4. Fornasini, F. M., etal. 2020, MNRAS, 495, 771
5. Fragos, T., et al. 2013, ApJ, 764, 41
6. Garner, Rob. 2017, "Messier 51 (the Whirlpool Galaxy)." *NASA*, NASA.
7. Hunt, Q., et al. 2021, arXiv:2102.07293
8. Kilgard, R. 2014, "Photo Album : Whirlpool Galaxy : June 3, 2014." *Chandra*, Chandra X-Ray Observatory.
9. Lopez, K. M., etal. 2019, MNRAS, 489, 1249
10. Lehmer, B.D., *et al.* 2016 *ApJ* **825** 7
11. Lehmer, B. D., et al. 2021, ApJ, 907,17
12. Lehmer, B. D., et al. 2010, ApJ, 724, 559
13. Linden, T., et al. 2010, ApJ, 725, 1984
14. Markoff, Sera. 2020, Current Research Background.
15. Mineo, S., etal. 2012, MNRAS, 419, 2095
16. Pakull, M. W., etal. 2010, Nature, 466, 209
17. Remillard, R. A. & McClintock, J. E. 2006, ARAA, 44, 49
18. Shakura, N. I., & Sunyaev, R. A. 1973, A&A, 24, 337.
19. Soria, R., etal. 2010, MNRAS, 409, 541,
20. Vulic, N. et al. 2018 ApJ 864, 2
21. Wiktorowicz, G., etal. 2019, ApJ, 875, 53